

Accepted Manuscript

Synthesis and antitumor activity of novel substituted uracil-1'(N)-acetic acid ester derivatives of 20(S)-camptothecins

Di-Zao Li, Qiang-Zhe Zhang, Cun-Ying Wang, Yan-Ling Zhang, Xing-Yu Li, Ji-Tao Huang, Hong-Yan Liu, Zhao-Di Fu, Hua-Xian Song, Jin-Ping Lin, Teng-Fei Ji, Xian-Dao Pan

PII: S0223-5234(16)30951-5

DOI: [10.1016/j.ejmech.2016.11.013](https://doi.org/10.1016/j.ejmech.2016.11.013)

Reference: EJMECH 9046

To appear in: *European Journal of Medicinal Chemistry*

Received Date: 1 August 2016

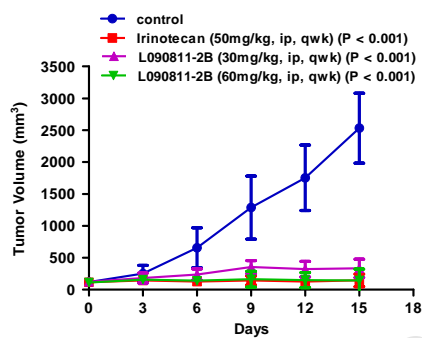
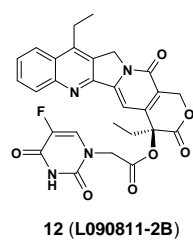
Revised Date: 30 October 2016

Accepted Date: 6 November 2016

Please cite this article as: D.-Z. Li, Q.-Z. Zhang, C.-Y. Wang, Y.-L. Zhang, X.-Y. Li, J.-T. Huang, H.-Y. Liu, Z.-D. Fu, H.-X. Song, J.-P. Lin, T.-F. Ji, X.-D. Pan, Synthesis and antitumor activity of novel substituted uracil-1'(N)-acetic acid ester derivatives of 20(S)-camptothecins, *European Journal of Medicinal Chemistry* (2016), doi: 10.1016/j.ejmech.2016.11.013.

This is a PDF file of an unedited manuscript that has been accepted for publication. As a service to our customers we are providing this early version of the manuscript. The manuscript will undergo copyediting, typesetting, and review of the resulting proof before it is published in its final form. Please note that during the production process errors may be discovered which could affect the content, and all legal disclaimers that apply to the journal pertain.





Synthesis and antitumor activity of novel substituted uracil-1'(N)-acetic acid ester derivatives of 20(S)-camptothecins

Di-Zao Li^{a,b,1}, Qiang-Zhe Zhang^{a,1}, Cun-Ying Wang^{c,1}, Yan-Ling Zhang^{d,1}, Xing-Yu Li^a, Ji-Tao Huang^a, Hong-Yan Liu^b, Zhao-Di Fu^b, Hua-Xian Song^e, Jin-Ping Lin^e, Teng-Fei Ji^{*b}, Xian-Dao Pan^{*b}

a: College of Pharmacy and State key Laboratory of Medicinal Chemical Biology, State Key Laboratory of Elemento-Organic Chemistry and Tianjin Key Laboratory of Molecular Drug Research, Nankai University, Tianjin 300071, P. R. China;

b: State Key Laboratory of Bioactive Substance and Function of Natural Medicines, Institute of Materia Medica, Chinese Academy of Medical Sciences and Peking Union Medical College, Beijing 100050, P. R. China;

c: Xu Zhou College of Industrial Technology, Xuzhou 221000, China;

d: School of Chemistry and Chemical Engineering, Inner Mongolia University, Hohhot, Inner Mongolia, 010021, P. R. China;

e: Beijing Landan Pharm, Beijing 100176, P. R. China.

* Corresponding Authors

E-mail addresses: xdp@imm.ac.cn (X. P.); jtif@imm.ac.cn (T. J.).

¹ These authors contributed equally to this work.

ABSTRACT:

A series of novel substituted uracil-1'(N)-acetic acid esters (**6–20**) of camptothecins (CPTs) were synthesized by the acylation method. These new compounds were evaluated for *in vitro* antitumor activity against tumor cell lines, A549, Bel7402, BGC-823, HCT-8 and A2780. *In vitro* results showed that most of the derivatives exhibited comparable or superior cytotoxicity compare to CPT (**1**) and topotecan (TPT, **2**), with **12** and **13** possessing the best efficacy. Four compounds, **9**, **12**, **13** and **16**, were selected to be evaluated for *in vivo* antitumor activity against H₂₂, BGC-823 and Bel-7402 in mice. *In vivo* testing results indicated that **12** and **13** had antitumor activity against mouse liver carcinoma H₂₂ close to Paclitaxel and cyclophosphamide. **12** had similar antitumor activity against human gastric carcinoma BGC-823 in nude mice compared to irinotecan (**3**) and possessed better antitumor activity against human hepatocarcinoma Bel-7402 in nude mice than **3**. It is also discovered that **12** showed a similar mechanism but better inhibitory activity on topoisomerase I (Topo I) compared to **2**. These findings indicate that 20(S)-O-fluorouracil-1'(N)-acetic acid ester derivative of CPTs, **12**, could be developed as an antitumor drug candidate for clinical trial.

Keywords: Camptothecin; Synthesis; Substituted uracil-1'(N)-acetic acid; Antitumor activity; the mechanism of antitumor activity

1. Introduction

Camptothecin (CPT, **1**, **Figure 1**) and its related analogues represent an important class of agents useful in the treatment of cancer [1–4]. Structure-activity relationship (SAR) studies showed that the ring E lactone and the natural 20*S*-configuration of camptothecins (CPTs) are essential for antitumor activity because of their topoisomerase I (Topo I) inhibitory activity (**Figure 2**). The modification of CPT on its A- and B-rings, such as topotecan (TPT, **2**, **Figure 1**), irinotecan (**3**, **Figure 1**), rubitecan (9-nitrocamptothecin, 9-NO₂-CPT, **4**, **Figure 1**), 10-hydroxycamptothecin and 7-ethyl-10-boronic acid camptothecin as prodrug of SN-38, the active metabolite of **3**, the typical Topo I inhibitors, could effectively ablate high-affinity binding of the carboxylate to human serum albumin (HSA), and improve antitumor activity of CPT [5–14].

Because of the stronger intramolecular hydrogen bonding in polar solvents, the 20(*S*)-hydroxyl group of CPT is believed to increase the reaction rate of lactone hydrolysis of CPT at neutral pH by shifting the equilibrium from the lactone form to the carboxylate form [15]. In this respect, esterification of 20-hydroxyl group is speculated to not only eliminate the intramolecular hydrogen bonding but also increase the steric hindrance of carbonyl group of E-ring [16]. Although 20-*O*-acylated CPTs possess no intrinsic Topo I inhibitory activity, they can be functioned as prodrugs to release the CPTs *in vivo*, and improve solubility, pharmacokinetics character and safety of CPTs [17]. A series of 20-*O*-acylated CPT derivatives, such as 20-*O*-glycinate [18], 20-*O*-alkanoate [19], 20-*O*-aroylate [20], and 20-*O*-PG-glycinate [21], were prepared to improve stability and solubility of lactone in CPT. Oxyalkanoic acid esters and nitrogen-based esters of CPT were synthesized previously, and these esters showed significant antitumor activity and low toxicity *in vivo* [16, 22]. Another series of nitrogen-based esters of CPT, 20(*S*)-sulfonylamidine derivatives of **1**, were investigated as potential anticancer agents directly and selectively inhibiting Topo I [23, 24]. These results validated our hypothesis on SAR of CPT [25–27]. Based on this SAR, we designed a series of novel substituted uracil-1'(*N*)-acetic acid esters of CPTs to improve their antitumor activity. Herein substituted uracil-1'(*N*)-acetic acid esters of CPTs as new compounds were prepared and evaluated for their *in vitro* and *in vivo* antitumor activity.

2. Results and discussion

2.1. Chemistry

To study the antitumor activity of the different substituent groups on 5'-position of uracil-1'(*N*)-acetic acid esters of CPTs, we synthesized a series of CPT derivatives (**6–20**) containing H, F, Cl, Br, and I group on 5'-position of uracil. Preparation (**Scheme 1**) and purification of 1'(*N*)-acetic acid **5a–e** were performed according to previously published procedures [28]. CPTs' ester derivatives **6–20** were prepared in proper yields by the straightforward acylation of CPTs like **1**, 9-NO₂-CPT or 7-ethylcamptothecin (7-Et-CPT) with the corresponding substituted uracil-1'(*N*)-acetic acid in the presence of a coupling agent 1-[3-(dimethylamino) propyl]-3-ethylcarbodiimide hydrochloride (EDCI) and a catalyst 4-dimethylaminopyridine (DMAP) in dried pyridine at room temperature (r.t.) [29] (**Scheme 1**).

2.2. In Vitro Cytotoxicity Assay

Cytotoxic activity of these CPTs-20-*O*-ester derivatives was evaluated against five human tumor cell lines, A549, Bel7402, BGC-823, HCT-8, and A2780, by using the MTT assay (**Table 1**) according to the previous method [20, 30]. CPT and TPT were used as comparisons. CPT possessed excellent antitumor activities *in vitro* in nanomolar concentration, and higher cytotoxic activity than TPT. These ester compounds showed comparable or higher cytotoxic activity compared to TPT. Most of these compounds displayed less cytotoxicity compared to CPT. The data exhibiting cytotoxicity of ester were related to that of its parent compound. The ester **6, 8, 9, 11, 12, 13, 14, 16, 17, 18, 19** and **20** had cytotoxic activity (IC_{50} 0.002–0.032 μ M) higher than TPT (IC_{50} 0.022–0.100 μ M) and comparable to or even slightly better than CPT (IC_{50} 0.014–0.057 μ M) on Bel7402, BGC-823 and HCT-8. The cytotoxic activity of ester **11** and **16** on A2780, were similar to that of TPT.

The cytotoxicity of the CPT ester could be explained by the structure of heterocyclic acid of uracil and the substituents on the CPT. The ester containing ethyl or nitro-group on the CPT and F, Cl, and Br on the 5-position of uracil may strengthen the cytotoxicity, as **12, 13** and **16** possessed the best cytotoxicity. In contrast, the ester containing iodine atom on the 5-position of uracil might weaken the cytotoxicity because **10** and **15** showed the weakest cytotoxic activity in all compounds tested with IC_{50} values almost in micro-molar per liter concentration level. That is perhaps because the steric hindrance or polarity of iodine is not conducive to form CPTs-DNA-Topo I complex.

2.3. *In Vivo* Antitumor Activity Assays

Considering the above analysis of cytotoxicity and structures of the ester derivatives synthesized, four of these compounds, **9, 12, 13** and **16**, were selected to evaluate their *in vivo* antitumor activity in mice by intra peritoneal injection, and the tumor model was mouse liver tumor H₂₂ model.

In vivo preliminary evaluation of toxicity and antitumor activity of analogues **9, 12, 13** and **16** were performed on KM (Kun Ming of China) mice (**Table 2**). The data revealed that compound **12** and **13** possessed higher tumor inhibitory rate (TIR, 57.51% and 46.21%) against H₂₂ transplanted mice tumor than that of **16** (11.0%) and **9** (6.39%), lower than that of paclitaxel (73.85%). However, all four esters tested showed lower toxicity in the dose of 40 mg/kg for twice than that of paclitaxel in the dose of 24 mg/kg for three times. In view of these facts, compounds **12** and **13** were further investigated for their doses to be used safely.

During the further investigation of *in vivo* antitumor activity with different doses (**Table 3**), both **12** and **13** showed a better dose-efficacy relationship. The *in vivo* antitumor activity results also showed that TIRs of **13** were higher than that of **12** in same doses (58.68% vs. 39.12% in 100 mg/kg for once, 76.58% vs. 64.46% in 60 mg/kg for twice), but TIRs in 60mg/kg for twice were lower than that of cyclophosphamide (93.66%). Compound **13** possessed higher TIR, but its toxicity was higher than that of **12**, with three out of ten mice died when treated by the dose of 60 mg/kg twice. Therefore, the compound **12** was selected as the candidate compound for further investigation of antitumor test.

Further evaluations of antitumor activity *in vivo* showed that **12** had almost same antitumor activity (TIR: 95.97%, T/C: 5.54%, 60mg/kg for twice without death of animals) against human gastric cancer BGC-823 in nude mice compared to irinotecan (TIR: 94.10%, T/C: 5.48%) (**Table 4, Table 5, and Figure 3**). Ester **12** possessed better antitumor activity and lower toxicity (TIR: 81.45%, T/C: 24.53%, 60 mg/kg for twice) against human liver

carcinoma Bel-7402 in nude mice than that of TPT (TIR: 45.48%, T/C: 58.80%, 5 mg/kg for twice) (**Table 6, 7, and Figure 4**).

2.4. Mechanism of Action Studies on Compound **12**

Two separate assays were carried out to explore the mode of action of compound **12** and TPT. **12** was preferentially tested for Topo I inhibitory activity using topotecan as a reference drug [31–33]. As shown in **Figure 5**, compounds **12** exhibited strong Topo I inhibitory activity with an almost equal potency compared to TPT with a concentration leading to an inhibition of Topo I from 30 μ M. Because a typical characteristic of TPT is the ability to induce cell cycle arrest at G2/M phase [23, 34], we assessed perturbation of the cell cycle on A549 cell using flow cytometry. It is found that treatment of compound **12** at concentrations from 8 nM to 75 nM caused a marked increase in the proportion of G2/M phase cells from around 10% to 71.7% (**Figure 6**). Moreover, compound **12** showed better Topo I inhibitory effect than TPT.

To study the mechanism of antitumor activity, the apoptosis profile of A-549 human lung adenocarcinoma epithelial cells treated by **12** was investigated. Firstly, morphological cellular changes of A-549 cells treated with compound **12** at concentrations from 8 nM to 75 nM were studied. The treated cells showed apoptotic morphological features, including cell shrinkage and membrane blebbing in concentration-dependent manners (**Figure 7A**). Next, the apoptosis by double staining with FITC-annexin V and propidium iodide was confirmed. The result of flow cytometry indicated that **12** treatment at concentrations from 8 nM to 75 nM increased the percentage of apoptotic cells from around 3% to 59% (**Figure 7B**). The protein of apoptosis signal pathway by western blot was also studied, showing that anti-apoptotic protein Bcl-2 [35] was reduced, while apoptotic protein Bax [36] and cleaved Caspase-3 with **12** treatment were enhanced at concentrations from 8 nM to 75 nM from the proteins without **12** treatment (**Figure 7C**). These data demonstrated that **12** inhibited A-549 cell growth through apoptosis induction.

3. Conclusion

Fifteen novel substituted uracil-1'(N)-acetic acid esters of camptothecins were prepared according to a known method. The in vitro cytotoxicity was evaluated on five human cancer cell lines (A549, Bel7402, BGC-823, HCT-8, and A2780) by using a MTT assay. In vivo antitumor activity showed that compound **12** possessed higher tumor inhibitory activity and lower toxicity compared to TPT. The mechanism study revealed that ester **12** was a Topo I inhibitor (the same as TPT). Compound **12** showed significantly higher in vivo antitumor activity and lower toxicity compared with TPT, and similar TIR compared to irinotecan. Therefore, it is definitely warranted that compound **12** is a new class of Topo I inhibitor and antitumor clinical trial drug candidate of CPTs.

4. Experimental section

4.1. Chemistry

All reactions requiring anhydrous conditions were performed under an Ar or N₂ atmosphere. Chemicals and solvents were either A.R. grade or purified by standard techniques. Flash column chromatography was carried out on silica gel 300–400 mesh. Column chromatography was performed by using silica gel with eluent given in parentheses. Thin layer chromatography (TLC) analyses were carried out on silica gel plates GF₂₅₄ (Qingdao Haiyang Chemical Co., Ltd.), compounds were visualized by irradiation with UV light. Melting points were determined in Yanaco melting point apparatus and are uncorrected. The NMR and MS (ESI) spectra of these compounds were consistent with their structures. NMR analyses were performed on a Bruker instrument AV 400 (Bruker Company, USA) by using CDCl₃ or DMSO-*d*₆ as a solvent with tetramethylsilane (TMS) as reference at room temperature. ¹H NMR spectra were recorded at 400 MHz and chemical shifts (δ values) are reported in parts per million (ppm) relative to either a TMS (δ = 0.00 ppm) internal standard or solvent signals and coupling constants (*J* values) are given in Hz, respectively. ¹³C NMR spectra were recorded at 100 MHz and chemical shifts (δ values) are reported in ppm measured relative to the solvent peak. MS (ESI) spectra were recorded on Finnigan Lcqd advantage instrument. High-resolution mass spectra (HRMS) were obtained with a VG ZAB-HS spectrometer.

The purity of compound **12** was analyzed compared with 7-Et-CPT by reverse-phase HPLC instrument Agilent 1100 with Kromasil C18 column (250×4.6mm, 5 μ m), detection wavelength 256nm, column temperature 25 °C, and their relative contents were determined by normalization method of area (**Figure 8**). Specific optical rotation of compound **12** was determined by SGW-5 automatic polarimeter, Shanghai, at 20 °C.

4.2. Synthesis of Key Intermediates **5a–e**.

Potassium hydroxide (40.0 mmol) was stirred to be dissolved in distilled water (10 mL) at r.t. and the appropriate uracil or 5'-substituted uracil (10.0 mmol) was added portionwise with vigorous stirring until the mixture was well-distributed, and then the mixture was heated at 60 °C for 0.5–1 h to be a clear solution. To this solution, the solution of bromoacetic acid (12.1–14.5 mmol) in distilled water (8 mL) was added dropwise over 30 minutes. The reaction mixture was heated at 60 °C for another 5 h and was allowed to cool to r.t.. The mixture was acidified to pH 2 with concentrated HCl aqueous solution and stirred overnight. The resulting precipitate was collected by filtration to yield a white or pale yellow solid, which was recrystallized from the minimal amount of distilled water to afford the *title compound*, an *N*-acetic acid derivative of the uracils **5a–e** in 60-90% yield.

4.3. General Synthetic Procedure for Compounds **6–20**.

The corresponding uracil or 5'-substituted uracil 1'(*N*)-acetic acid, one of the key intermediates **5a–e** (1.2 mmol), was dissolved in 20 mL of anhydrous pyridine which had been pre-treated by 4Å molecular sieves and KOH more than 48 hours at rt. To this solution, EDCI (1.5 mmol) and DMAP (0.2–0.6 mmol) were added slowly at 0 °C, and this mixture was stirred for 10 minutes or some longer time until a clear solution was obtained. Under an N₂ atmosphere, CPTs like CPT, 9-NO₂-CPT or 7-Et-CPT (0.4 mmol) was added in one portion. The reaction mixture was allowed to warm to r.t. and stirred for 12–36 h. After the reaction was completed, as monitored by TLC, the reaction mixture was diluted by adding CH₂Cl₂ (40 mL) and aqueous 1 N HCl solution (30 mL). The mixture was stirred for an additional 30 min, and two layers were separated. The aqueous layer was extracted with CH₂Cl₂ (30

mL × 3). The combined organic layers were dried over Na₂SO₄, filtered, and concentrated in vacuo. The crude residue was purified by flash column chromatography on Silicon gel with CHCl₃-MeOH (10:1–20:1) as eluent to give **6–20**. NMR spectra of all the new compounds **6–20** are provided as Supporting Information.

4.3.1. Compound **6**

Pale yellow solid; yield 84.6%; mp 278–281 °C; ¹H NMR (400 MHz, DMSO-*d*₆, TMS) δ: 11.41 (s, 1H, NH), 8.70 (s, 1H, Ar-H), 8.18 (d, *J* = 8.4 Hz, 1H, Ar-H), 8.13 (d, *J* = 8.0 Hz, 1H, Ar-H), 7.88 (t, *J* = 8.0 Hz, 1H, Ar-H), 7.73 (t, *J* = 7.6 Hz, 1H, Ar-H), 7.67 (d, *J* = 8.0 Hz, 1H, 6'-H), 7.22 (s, 1H, Ar-H), 5.62 (d, *J* = 7.6 Hz, 1H, 5'-H), 5.51 (s, 2H, H-17), 5.31 (d, *J* = 3.2 Hz, 2H, H-5), 4.83 (dd, *J* = 38.4, 17.6 Hz, 2H, OOCCH₂-N), 2.16 (q, *J* = 7.2 Hz, 2H, 19-CH₂), 0.91 (t, *J* = 7.2 Hz, 3H, 18-CH₃); ¹³C NMR (100MHz, DMSO-*d*₆, TMS) δ: 167.9, 167.3, 164.1, 157.0, 152.9, 151.3, 148.4, 146.5, 146.0, 132.0, 130.9, 130.3, 129.5, 129.1, 129.0, 128.5, 128.2, 119.4, 101.8, 95.7, 77.4, 66.8, 50.7, 48.8, 30.8, 7.9; HRMS (ESI): *m/z* calcd for C₂₆H₂₀N₄O₇+H 501.1405, found 501.1404.

4.3.2. Compound **7**

Pale yellow solid; yield 86.6%, m p 274–276 °C; ¹H NMR (400MHz, DMSO-*d*₆, TMS) δ: 11.98 (d, *J* = 1.6 Hz, 1H, NH), 8.70 (s, 1H, Ar-H), 8.17 (m, 3H, 2×Ar-H & 6'-H), 7.89 (m, 1H, Ar-H), 7.73 (m, 1H, Ar-H), 7.22 (s, 1H, Ar-H), 5.52 (d, *J* = 2.0 Hz, 2H, H-17), 5.31 (d, *J* = 4.0 Hz, 2H, H-5), 4.77 (dd, *J* = 38.0, 17.6 Hz, 2H, OOCCH₂-N), 2.17 (dd, *J* = 14.8, 7.2 Hz, 2H, 19-CH₂), 0.91 (t, *J* = 7.6 Hz, 3H, 18-CH₃); ¹³C NMR (100MHz, DMSO-*d*₆, TMS) δ: 168.0, 167.1, 166.7, 156.4, 152.4, 149.5, 147.9, 146.0, 144.6, 133.8, 131.5, 130.4, 129.8, 129.0, 128.5, 128.0, 127.7, 118.9, 115.4, 95.2, 77.0, 66.3, 50.2, 48.4, 30.3, 7.4; MS (ESI): *m/z* 1035 (2M-H)⁻; HRMS (ESI): *m/z* calcd for C₂₆H₁₉FN₄O₇+H 519.1311, found 519.1302.

4.3.3. Compound **8**

Pale yellow solid; yield 85.0%; mp 252–254 °C; ¹H NMR (400 MHz, DMSO-*d*₆, TMS) δ: 12.00 (s, 1H, NH), 8.70 (s, 1H, Ar-H), 8.25 (s, 1H, 6'-H), 8.18 (m, 2H, Ar-H), 7.89 (t, *J* = 7.2 Hz, 1H, Ar-H), 7.73 (t, *J* = 7.2 Hz, 1H, Ar-H), 7.23 (s, 1H, Ar-H), 5.52 (s, 2H, H-17), 5.30 (d, *J* = 4.0 Hz, 2H, H-5), 4.77 (dd, *J* = 33.2, 17.6 Hz, 2H, OOCCH₂-N), 2.17 (dd, *J* = 14.8, 7.6 Hz, 2H, 19-CH₂), 0.91 (t, *J* = 7.6 Hz, 3H, 18-CH₃); ¹³C NMR (100 MHz, DMSO-*d*₆, TMS) δ: 167.0, 166.7, 159.3, 156.4, 152.4, 149.9, 147.9, 146.0, 144.5, 142.6, 131.5, 130.4, 129.8, 129.0, 128.5, 128.0, 127.7, 118.9, 106.5, 95.2, 77.0, 66.3, 50.2, 48.5, 30.3, 7.4; MS (ESI): *m/z* 1067 (2M-H)⁻; HRMS (ESI): *m/z* calcd for C₂₆H₁₉ClN₄O₇+H 535.1015, found 535.1012.

4.3.4. Compound **9**

Pale yellow solid; yield 82.0%; mp 248–251 °C; ¹H NMR (400 MHz, DMSO-*d*₆, TMS) δ: 11.81 (s, 1H, NH), 8.69 (s, 1H, Ar-H), 8.29 (s, 1H, 6'-H), 8.18 (m, 2H, Ar-H), 7.88 (t, *J* = 8.0 Hz, 1H, Ar-H), 7.73 (t, *J* = 7.6 Hz, 1H, Ar-H), 7.22 (s, 1H, Ar-H), 5.51 (s, 2H, H-17), 5.30 (d, *J* = 3.2 Hz, 2H, H-5), 4.87 (dd, *J* = 33.6, 17.6 Hz, 2H, OOCCH₂-N), 2.17 (dd, *J* = 14.8, 7.2 Hz, 2H, 19-CH₂), 0.91 (t, *J* = 7.2 Hz, 3H, 18-CH₃); ¹³C NMR (100MHz, DMSO-*d*₆, TMS) δ: 167.2, 166.7, 160.9, 156.4, 152.3, 150.5, 149.6, 147.9, 146.0, 144.5, 131.5, 130.4, 129.8, 129.0,

128.5, 127.9, 127.7, 118.9, 95.2, 77.0, 68.5, 66.3, 50.2, 48.3, 30.4, 7.4; MS (ESI): m/z 1251 (2M-H)⁻; HRMS (ESI): m/z calcd for C₂₆H₁₉IN₄O₇+H 627.0371, found 627.0376.

4.3.5. Compound 10

Pale yellow solid; yield 84.0%; mp 238–240 °C; ¹H NMR (400 MHz, DMSO-*d*₆, TMS) δ : 11.96 (s, 1H, NH), 8.69 (s, 1H, Ar-H), 8.32 (s, 1H, 6'-H), 8.18 (m, 2H, Ar-H), 7.88 (t, J = 7.6 Hz, 1H, Ar-H), 7.73 (t, J = 7.2 Hz, 1H, Ar-H), 7.22 (s, 1H, Ar-H), 5.51 (s, 2H, H-17), 5.29 (d, J = 3.2 Hz, 2H, H-5), 4.84 (dd, J = 33.2, 17.6 Hz, 2H, OOCCH₂-N), 2.17 (dd, J = 14.4, 7.2 Hz, 2H, 19-CH₂), 0.92 (t, J = 7.2 Hz, 3H, 18-CH₃); ¹³C NMR (400 MHz, DMSO-*d*₆, TMS) δ : 167.1, 166.7, 159.5, 156.4, 152.3, 150.1, 147.9, 146.0, 145.0, 144.5, 131.5, 130.4, 129.8, 129.0, 128.5, 127.9, 127.7, 118.9, 95.2, 94.9, 77.0, 66.4, 50.2, 48.5, 30.3, 7.4; HRMS (ESI): m/z calcd for C₂₆H₁₉BrN₄O₇+H 579.0510, found 579.0513.

4.3.6. Compound 11

Pale yellow solid; yield 86.6%; mp 260–262 °C; ¹H NMR (400 MHz, DMSO-*d*₆, TMS) δ : 11.41 (s, 1H, NH), 8.25 (d, J = 8.4 Hz, 1H, Ar-H), 8.17 (d, J = 8.4 Hz, 1H, Ar-H), 7.86 (t, J = 7.2 Hz, 1H, Ar-H), 7.73 (t, J = 7.6 Hz, 1H, Ar-H), 7.69 (d, J = 8.0 Hz, 1H, 6'-H), 7.20 (s, 1H, Ar-H), 5.63 (d, J = 7.6 Hz, 1H, 5'-H), 5.53 (s, 2H, H-17), 5.30 (dd, J = 25.6, 18.8 Hz, 2H, H-5), 4.84 (dd, J = 37.2, 17.6 Hz, 2H, OOCCH₂-N), 3.20 (d, J = 7.2 Hz, 2H, 7-CH₂Me), 2.18 (d, J = 7.2 Hz, 2H, 19-CH₂), 1.30 (t, J = 6.8 Hz, 3H, 7-CH₂CH₃), 0.93 (t, J = 6.8 Hz, 3H, 18-CH₃); ¹³C NMR (100MHz, DMSO-*d*₆, TMS) δ : 167.4, 166.8, 163.6, 156.4, 151.7, 150.8, 148.4, 146.6, 145.5, 145.4, 144.7, 129.9, 129.8, 127.9, 127.6, 126.5, 124.0, 118.8, 101.3, 95.1, 76.9, 66.3, 49.4, 48.3, 30.3, 22.1, 13.9, 7.4; MS (ESI): m/z 529 (M+H)⁺, 1057 (2M+H)⁺, 1079 (2M+Na)⁺; HRMS (ESI): m/z calcd for C₂₈H₂₄N₄O₇+H 529.1718, found 529.1727.

4.3.7. Compound 12

Yellow solid; yield 88.0%; mp > 270 °C (dec.); purity by HPLC 97.3% (flow rate 1.0ml/min, mobile phase MeOH:H₂O 59:41); Specific optical rotation [α] -63.2° (in CHCl₃, c = 9.2×10⁻³ M); ¹H NMR (400 MHz, DMSO-*d*₆, TMS) δ : 12.00 (s, 1H, NH), 8.17 (m, 3H, 2×Ar-H & 6'-H), 7.85 (t, J = 7.6 Hz, 1H, Ar-H), 7.71 (t, J = 7.6 Hz, 1H, Ar-H), 7.21 (s, 1H, Ar-H), 5.55 (s, 2H, H-17), 5.25 (d, J = 6.4 Hz, 2H, H-5), 4.80 (dd, J = 36.8, 17.6 Hz, 2H, OOCCH₂-N), 3.16 (d, J = 6.8 Hz, 2H, 7-CH₂Me), 2.20 (d, J = 7.2 Hz, 2H, 19-CH₂), 1.29 (t, J = 7.2 Hz, 3H, 7-CH₂CH₃), 0.95 (t, J = 7.2 Hz, 3H, 18-CH₃); ¹³C NMR (100MHz, DMSO-*d*₆, TMS) δ : 167.1, 166.7, 157.5, 157.2, 156.4, 151.6, 149.5, 148.4, 146.5, 145.5, 144.6, 129.9, 129.8, 129.7, 127.8, 127.5, 126.4, 123.9, 118.8, 95.1, 77.0, 66.3, 49.4, 48.4, 30.3, 22.1, 13.9, 7.4; MS (ESI): m/z 547 (M+H)⁺, 1093 (2M+H)⁺, 1115 (2M+Na)⁺, 545 (M-H)⁻, 1091 (2M-H)⁻; HRMS (ESI): m/z calcd for C₂₈H₂₃FN₄O₇+H 547.1624, found 547.1632.

4.3.8. Compound 13

Pale yellow solid; yield 84.0%; mp 275–277 °C (dec.); ¹H NMR (400MHz, DMSO-*d*₆, TMS) δ : 12.00 (s, 1H,

NH), 8.26 (d, $J = 8.4$ Hz, 1H, Ar-H), 8.25 (s, 1H, 6'-H), 8.17 (d, $J = 8.4$ Hz, 1H, Ar-H), 7.86 (t, $J = 7.6$ Hz, 1H, Ar-H), 7.73 (t, $J = 8.0$ Hz, 1H, Ar-H), 7.21 (s, 1H, Ar-H), 5.53 (s, 2H, H-17), 5.32 (d, $J = 6.8$ Hz, 2H, H-5), 4.84 (dd, $J = 32.4, 17.6$ Hz, 2H, OOCCH₂-N), 3.22 (dd, $J = 14.4, 7.2$ Hz, 2H, 7-CH₂Me), 2.18 (dd, $J = 14.0, 6.4$ Hz, 2H, 19-CH₂), 1.30 (t, $J = 7.2$ Hz, 3H, 7-CH₂CH₃), 0.92 (t, $J = 7.2$ Hz, 3H, 18-CH₃); ¹³C NMR (100 MHz, DMSO-*d*₆, TMS) δ : 167.0, 166.7, 159.3, 156.4, 151.7, 149.9, 148.4, 146.6, 145.5, 144.5, 142.6, 130.0, 129.8, 127.9, 127.6, 126.5, 124.0, 118.8, 106.5, 95.1, 77.0, 66.4, 49.5, 48.5, 30.3, 22.1, 13.9, 7.4; MS (ESI): m/z 563 (M+H)⁺, 1125 (2M+H)⁺, 1147 (2M+Na)⁺, 561 (M-H)⁻, 1123 (2M-H)⁻; HRMS (ESI): m/z calcd for C₂₈H₂₃FN₄O₇+H 563.1328, found 563.1333.

4.3.9. Compound 14

Pale yellow solid; yield 80.0%; mp 257–259 °C; ¹H NMR (400 MHz, DMSO-*d*₆, TMS) δ : 11.83 (s, 1H, NH), 8.30 (s, 1H, 6'-H), 8.23 (d, $J = 5.6$ Hz, 1H, Ar-H), 8.18 (d, $J = 8.0$ Hz, 1H, Ar-H), 7.85 (t, $J = 7.6$ Hz, 1H, Ar-H), 7.71 (t, $J = 8.0$ Hz, 1H, Ar-H), 7.20 (s, 1H, Ar-H), 5.54 (s, 2H, H-17), 5.26 (s, 2H, H-5), 4.84 (dd, $J = 31.6, 17.6$ Hz, 2H, OOCCH₂-N), 3.18 (m, 2H, 7-CH₂Me), 2.19 (m, 2H, 19-CH₂), 1.29 (t, $J = 7.2$ Hz, 3H, 7-CH₂CH₃), 0.93 (t, $J = 7.2$ Hz, 3H, 18-CH₃); ¹³C NMR (100 MHz, DMSO-*d*₆, TMS) δ : 167.2, 166.7, 160.9, 156.4, 151.7, 150.5, 149.6, 148.4, 146.5, 145.5, 144.6, 129.9, 129.8, 127.8, 127.5, 126.5, 123.9, 118.8, 95.2, 77.0, 68.5, 66.4, 49.4, 48.3, 30.4, 22.1, 13.9, 7.4; MS (ESI): m/z 655 (M+H)⁺, 1309 (2M+H)⁺; 653 (M-H)⁻, 1307 (2M-H)⁻; HRMS (ESI): m/z calcd for C₂₈H₂₃FN₄O₇+H 655.0684, found 655.0691.

4.3.10. Compound 15

Pale yellow solid; yield 86.6%; mp > 280 °C (dec.); ¹H NMR (400 MHz, DMSO-*d*₆, TMS) δ : 11.96 (s, 1H, NH), 8.32 (s, 1H, 6'-H), 8.27 (d, $J = 7.6$ Hz, 1H, Ar-H), 8.17 (d, $J = 8.0$ Hz, 1H, Ar-H), 7.86 (t, $J = 7.6$ Hz, 1H, Ar-H), 7.73 (t, $J = 6.8$ Hz, 1H, Ar-H), 7.21 (s, 1H, Ar-H), 5.53 (s, 2H, H-17), 5.30 (s, 2H, H-5), 4.84 (dd, $J = 31.6, 17.6$ Hz, 2H, OOCCH₂-N), 3.21 (m, 2H, 7-CH₂Me), 2.18 (m, 2H, 19-CH₂), 1.30 (t, $J = 7.2$ Hz, 3H, 7-CH₂CH₃), 0.92 (t, $J = 7.2$ Hz, 3H, 18-CH₃); ¹³C NMR (100 MHz, DMSO-*d*₆, TMS) δ : 167.1, 166.7, 159.5, 156.4, 151.7, 150.1, 148.4, 146.6, 145.5, 145.0, 144.5, 129.9, 129.8, 127.9, 127.6, 126.5, 124.0, 118.8, 95.2, 94.9, 77.0, 66.4, 49.5, 48.5, 30.3, 22.1, 13.9, 7.4; HRMS (ESI): m/z calcd for C₂₈H₂₃FN₄O₇+H 607.0823, found 607.0824.

4.3.11. Compound 16

Dark yellow solid; yield 82.0%; mp > 250 °C (dec.); ¹H NMR (400 MHz, DMSO-*d*₆, TMS) δ : 11.43 (s, 1H, NH), 9.16 (s, 1H, Ar-H), 8.55 (t, $J = 8.0$ Hz, 2H, Ar-H), 8.05 (t, $J = 8.4$ Hz, 1H, Ar-H), 7.69 (d, $J = 8.0$ Hz, 1H, 6'-H), 7.28 (s, 1H, Ar-H), 5.63 (dd, $J = 7.6, 2.0$ Hz, 1H, 5'-H), 5.53 (d, $J = 2.0$ Hz, 2H, H-17), 5.35 (dd, $J = 26.8, 20.0$ Hz, 2H, H-5), 4.83 (dd, $J = 39.2, 17.6$ Hz, 2H, OOCCH₂-N), 2.16 (dd, $J = 15.2, 7.2$ Hz, 2H, 19-CH₂), 0.92 (t, $J = 7.2$ Hz, 3H, 18-CH₃); ¹³C NMR (100 MHz, DMSO-*d*₆, TMS) δ : 167.4, 166.7, 163.6, 156.4, 153.8, 150.8, 147.8, 145.9, 145.5, 145.1, 144.6, 135.8, 132.8, 129.0, 127.1, 125.5, 120.1, 119.9, 101.3, 96.1, 76.8, 66.3, 50.7, 48.3, 30.3, 7.4; MS (ESI): m/z 544 (M-H)⁻, 580 (M+Cl)⁻, 1089 (2M-H)⁻, 1125 (2M+Cl)⁻; HRMS (ESI): m/z calcd for C₂₆H₁₉N₅O₉+H 546.1256, found 546.1259.

4.3.12. Compound 17

Bright yellow solid; yield 86.5%; mp 235–237 °C; ¹H NMR (400 MHz, DMSO-*d*₆, TMS) δ: 12.00 (s, 1H, NH), 9.17 (s, 1H, Ar-H), 8.55 (dd, *J* = 7.6, 5.6 Hz, 2H, Ar-H), 8.17 (d, *J* = 6.4 Hz, 1H, 6'-H), 8.05 (t, *J* = 8.4 Hz, 1H, Ar-H), 7.28 (s, 1H, Ar-H), 5.54 (dd, *J* = 20.0, 17.2 Hz, 2H, H-17), 5.35 (dd, *J* = 27.2, 20.0 Hz, 2H, H-5), 4.77 (dd, *J* = 38.4, 17.6 Hz, 2H, OOCCH₂-N), 2.17 (dd, *J* = 14.8, 7.6 Hz, 2H, 19-CH₂), 0.92 (t, *J* = 7.2 Hz, 3H, 18-CH₃); ¹³C NMR (100 MHz, DMSO-*d*₆, TMS) δ: 167.1, 166.6, 157.2, 156.3, 153.8, 149.5, 147.8, 145.9, 145.1, 144.5, 138.3, 135.7, 132.8, 129.7, 129.0, 127.1, 125.5, 120.1, 119.9, 96.1, 76.9, 66.3, 50.7, 48.5, 30.3, 7.4; MS (ESI): *m/z* 562 (M-H)⁻, 598 (M+Cl)⁻, 1125 (2M-H)⁻, 1223 (2M+HSO₄)⁻; HRMS (ESI): *m/z* calcd for C₂₆H₁₈FN₅O₉+H 564.1161, found 564.1169.

4.3.13. Compound 18

Bright yellow solid; yield 83.0%; mp 242–244 °C; ¹H NMR (400 MHz, DMSO-*d*₆, TMS) δ: 12.01 (s, 1H, NH), 9.17 (s, 1H, Ar-H), 8.55 (t, *J* = 7.2 Hz, 2H, Ar-H), 8.25 (s, 1H, 6'-H), 8.05 (t, *J* = 8.0 Hz, 1H, Ar-H), 7.29 (s, 1H, Ar-H), 5.53 (dd, *J* = 20.0, 17.2 Hz, 2H, H-17), 5.36 (dd, *J* = 26.8, 19.6 Hz, 2H, H-5), 4.87 (dd, *J* = 34.0, 17.6 Hz, 2H, OOCCH₂-N), 2.19 (dd, *J* = 14.8, 6.8 Hz, 2H, 19-CH₂), 0.92 (t, *J* = 7.2 Hz, 3H, 18-CH₃); ¹³C NMR (100 MHz, DMSO-*d*₆, TMS) δ: 167.0, 166.6, 159.3, 156.3, 153.8, 149.9, 147.8, 145.9, 145.1, 144.5, 142.6, 135.8, 132.9, 129.0, 127.1, 125.5, 120.1, 119.9, 106.5, 96.1, 77.0, 66.3, 50.8, 48.5, 30.3, 7.4; MS (ESI): *m/z* 578 (M-H)⁻, 614 (M+Cl)⁻, 1157 (2M-H)⁻, 1255 (2M+HSO₄)⁻; HRMS (ESI): *m/z* calcd for C₂₆H₁₈ClN₅O₉+H 580.0866, found 580.0868.

4.3.14. Compound 19

Bright yellow solid; yield 82.6%; mp 252–254 °C; ¹H NMR (400 MHz, DMSO-*d*₆, TMS) δ: 11.82 (s, 1H, NH), 9.16 (s, 1H, Ar-H), 8.54 (t, *J* = 8.0 Hz, 2H, Ar-H), 8.29 (s, 1H, 6'-H), 8.04 (t, *J* = 8.0 Hz, 1H, Ar-H), 7.28 (s, 1H, Ar-H), 5.53 (dd, *J* = 20.4, 17.2 Hz, 2H, H-17), 5.35 (dd, *J* = 27.2, 20.0 Hz, 2H, H-5), 4.83 (dd, *J* = 34.0, 18.0 Hz, 2H, OOCCH₂-N), 2.17 (dd, *J* = 14.8, 7.2 Hz, 2H, 19-CH₂), 0.92 (t, *J* = 7.2 Hz, 3H, 18-CH₃); ¹³C NMR (100 MHz, DMSO-*d*₆, TMS) δ: 167.1, 166.6, 160.9, 156.3, 153.7, 150.5, 149.6, 147.8, 145.9, 145.1, 144.5, 135.8, 132.8, 129.0, 127.1, 125.5, 120.1, 119.9, 96.1, 76.9, 68.5, 66.3, 50.7, 48.3, 30.3, 7.4; MS (ESI): *m/z* 670 (M-H)⁻, 706 (M+Cl)⁻, 1341 (2M-H)⁻, 1377 (2M+Cl)⁻, 1439 (2M+HSO₄)⁻; HRMS (ESI): *m/z* calcd for C₂₆H₁₈IN₅O₉+H 672.0222, found 672.0224.

4.3.15. Compound 20

Bright yellow solid; yield 84.6%; mp 247–250 °C; ¹H NMR (400 MHz, DMSO-*d*₆, TMS) δ: 11.97 (s, 1H, NH), 9.17 (s, 1H, Ar-H), 8.55 (t, *J* = 7.2 Hz, 2H, Ar-H), 8.32 (s, 1H, 6'-H), 8.05 (t, *J* = 8.4 Hz, 1H, Ar-H), 7.28 (s, 1H, Ar-H), 5.53 (dd, *J* = 20.0, 16.8 Hz, 2H, H-17), 5.35 (dd, *J* = 26.8 Hz, 20.0 Hz, 2H, H-5), 4.83 (dd, *J* = 33.6, 17.6 Hz, 2H, OOCCH₂-N), 2.17 (dd, *J* = 14.8, 7.2 Hz, 2H, 19-CH₂), 0.92 (t, *J* = 7.6 Hz, 3H, 18-CH₃); ¹³C NMR (100 MHz, DMSO-*d*₆, TMS) δ: 167.0, 166.6, 159.5, 156.3, 153.8, 150.2, 147.8, 145.9, 145.1, 145.0, 144.5, 135.8, 132.9, 129.0,

127.1, 125.5, 120.1, 119.9, 96.1, 95.0, 76.9, 66.3, 50.8, 48.5, 30.3, 7.4; HRMS (ESI): m/z calcd for $C_{26}H_{18}BrN_5O_9+H$ 624.0361, found 624.0364.

4.4. Cell Lines and In Vitro Cytotoxicity Assays

The human tumor cell lines used in this work were A549 (lung carcinoma), Bel7402 (hepatocarcinoma), BGC-823 (gastric carcinoma), HCT-8 (colon cancer) and A2780 (ovarian cancer). These cell lines were obtained from the Peking Union Medical College (PUMC) in China. All cell lines were maintained and assayed in RPMI-1640 medium (GIBCO product) containing 10% heat-inactivated fetal bovine serum (bought from Hangzhou Sijiqing Biological Engineering Materials Co., Ltd.) in a humidified atmosphere containing 5% CO_2 in air. Compound stock solutions were prepared at 10 mM in DMSO and diluted with culture medium with the final DMSO concentration $\leq 0.01\%$ (v/v), a concentration without effect on cell growth. Cells were plated in 96-well microtiter plates at a density of $1-1.5 \times 10^3$ /well and incubated in a humidified atmosphere with 5% CO_2 at 37 °C for 24 h. Test compounds were added onto triplicate wells with different concentrations and 0.1% DMSO for control. After they had been incubated for 96 h, 100 μ L of MTT [3-(4,5-dimethylthiazol-2-yl)-2,5-diphenyltetrazolium bromide] (AMRESCO product) solution (0.4 mg/mL, prepared in RPMI1640) was added to each well and the plate was incubated for an additional 4 h. The supernatant was discarded before the formazan crystals were dissolved in 150 μ L of DMSO for each well. The absorbance (OD) was quantitated with microplate spectrophotometer (BIORAD type 550 enzyme mark instrument) at 540 nm with 405 nm as the reference wavelength. Wells containing no drugs were used as blanks for the spectrophotometer. The survival of the cells was expressed as percentage of untreated control wells. The IC_{50} (μ M) values, the concentrations which causing 50% inhibition of cell growth compared with that of the vehicle control, were determined according to the literatures' method [37, 38]. Compounds with $IC_{50} \leq 20 \mu$ M were considered effective. All the experiments were performed three times with duplicated samples.

4.5. Antitumor Activity in Vivo Assay on Compound **12**

The compounds were solved in normal saline using Tween-80 as the solubilizer. Four- to six-week-old BALB-c-nu male mice (Certificate SCXK-Jing-2009-0004, weighing 18–20 g) were obtained from Beijing Huafukang Bio-tech. Co., Ltd., PRC. Each of them was inoculated subcutaneously at the left flank with a tumor bulk of human gastric cancer BGC-823 or human liver carcinoma Bel-7402. The mice were divided into experimental groups after 6 days of inoculation. Groups ($n = 8$) consisted of control, Irinotecan or TPT and the analogue **12** with 30 mg/kg and 60 mg/kg two dose-groups. Mice received treatments, ip, at that day for the first time and then repeated the treatments once per week (QWK) to the end. The change of tumor volumes and body weights were observed and recorded every 3 days over the course of treatment. Tumor volumes (TV) were monitored by caliper measurement of the length and width and calculated using the formula of $TV = \frac{1}{2}ab^2$, where the “a” is the tumor length and the “b” is the width [32]. Mice were sacrificed on day 27–30 after implantation of

cells, and tumors were removed and recorded for analysis. Tumor inhibiting rate (%) was calculated when the control group's median tumor weight reached 1.0–1.4 g and compared with the treatment group's median tumor weight at that time. Relative tumor volumes (RTV) were calculated using the formula of $RTV = V_t / V_0$, where V_0 is the TV measured at the time of group-dividing and V_t is the TVs obtained every time from then on. The evaluation index of antitumor activity is the relative tumor growth rate T/C (%) with the calculating formula as followed,

$$T/C (\%) = [\text{Treatment Group (T) RTV} / \text{Negative Control Group (C) RTV}] \times 100\%$$

And the standard of curative effect evaluation is: $T/C (\%) > 40$, considered as invalid; $T/C (\%) \leq 40$, and after being subjected to the statistical dealing with the result of $P < 0.05$, considered as effective. Results were evaluated statistically by t-test [32].

4.6. Mechanism of Action Studies on Compound **12**

4.6.1. Morphological Observation

Morphological changes of culture cells were observed and examined by using a phase-contrast microscope and the photographs were taken by using a high-resolution digital camera (Nikon Eclipse Ti, Japan).

4.6.2. Apoptosis Assessment

Annexin V-FITC/propidium iodide double staining kit (BD Biosciences) was used to detect apoptosis. A549 cells (5×10^5 cells/mL) were seeded in six-well plates and treated with **12** at concentrations from 8 nM to 75 nM for 24 h. The cells were then harvested by trypsinization and washed for twice with ice-cold PBS. After centrifugation and removal of the supernatants, cells were resuspended in binding buffer which was then added to 5 μ L of annexin V-FITC and incubated at r.t. for 15 min. After adding 10 μ L of propidium iodide (PI) the cells were incubated at r.t. for another 15 min in the dark. The stained cells were analyzed by a flow cytometer (BD Dickinson) [32, 39].

4.6.3. Cell Cycle Arrest Assay

For flow cytometric analysis of cell cycle, A549 cells in exponential growth were treated with **12** and TPT with concentrations from 8 nM to 75 nM respectively for 48 h. The cells treated with **12** and TPT were collected, washed twice with PBS, and then fixed with 75% alcohol overnight. The cells were washed with PBS and eliminated the interference of RNA with 200 mg/mL RNase was added for 30 min. Then, the cells were staining with 20 mL/L propidium iodide (PI; Sigma) for 30 min. washed and the DNA content was detected by flow cytometer (BD Dickinson) [32, 39].

4.6.4. Western Blot Analysis

The treated cells with compound **12** were homogenized and subjected to SDS-PAGE. The proteins were transferred onto a polyvinylidene difluoride membrane (Roche Molecular Biochemicals, Quebec, Canada), blocked with 5% milk powder in TBS-T buffer (20 mM Tris-HCl, pH 7.4, 137 mM NaCl, and 0.1% Tween) for 1 h at r.t., incubated overnight at 4°C with appropriate primary antibodies against the target proteins, further incubated with HRP-conjugated secondary antibodies, and developed with the ECL System (Millipore, Billerica, MA).

4.6.5. Topo I-Mediated Plasmid DNA Pcmv-6 Relaxation Assay

DNA cleavage assay was performed as previously described [32, 33]. In brief, pcmv-6 DNA was incubated with Top I (New England Biolabs, American) in the presence or absence of indicated drugs, **12** and TPT, at 37 °C for 30 minutes and terminated by the addition of 10% sodium dodecylsulfate (SDS). Proteinase K (200 µg/mL final concentration) was added before the samples were incubated at 50 °C for 20 min. And 2 µL of 10× gel loading buffer (0.25% bromophenol blue, 50% glycerol) was added. The mixtures then were analyzed on a 1% agarose gel (containing 0.5 µg/mL ethidium bromide) at 8 V/cm for 1 h with TAE (Tris-Acetate-EDTA) as the running buffer. TPT was used as reference drug. The position of supercoiled DNA (SC) and relaxed DNA (RLX) were visualized with UV light and indicated with a Gel Doc Ez imager (Bio-Rad Laboratories, Ltd.).

Acknowledgments

This study was financially supported in part by the Fundamental Research Funds for the Central Universities of China (No. 65011141), the Research Fund for the Doctoral Program of Higher Education of China (Grant No. 20110031120048), the Natural Science Foundation of China (81672747), and Tianjin Municipality Science and Technology Commission (15JCYBJC50100).

Appendix A. Supplementary data

Supporting Information: NMR spectra of compounds **6–20**. This material is available free of charge via the Internet at <http://ees.elsevier.com>.

References

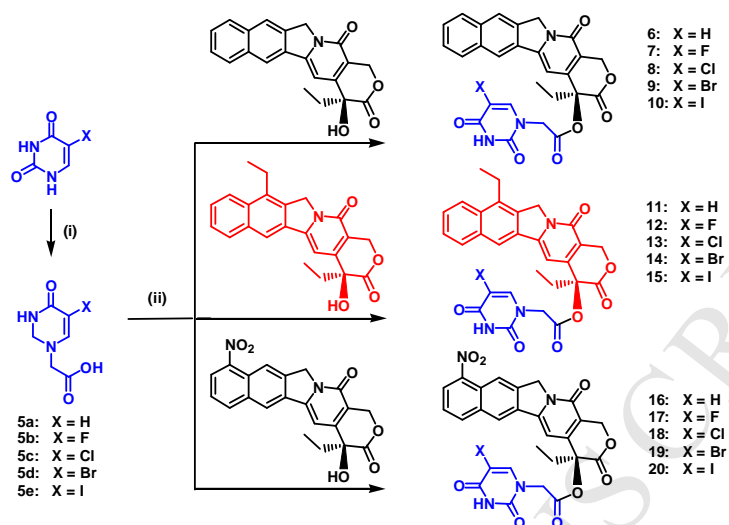
- [1] M.E. Wall, M.C. Wani, C.E. Cook, K.H. Palmer, A.T. McPhail, G.A. Sim, Plant antitumor agents I. The isolation and structure of camptothecin, a novel alkaloidal leukemia and tumor inhibitor from *Camptotheca acuminata*, *J. Am. Chem. Soc.* 88 (1966) 3888–3890.
- [2] H.K. Wang, S.L. Morris-Natschke, K.H. Lee, Antitumor agents 170. Recent advances in the discovery and development of topoisomerase inhibitors as antitumor agents, *Med. Res. Rev.* 17 (1997) 367–425 and literature cited therein.

- [3] N.H. Oberlies, D.J. Kroll, Camptothecin and taxol: historic achievements in natural products research, *J. Nat. Prod.* 67 (2004) 129–135.
- [4] K.H. Lee, Current development in the discovery and design of new drug candidates from plant natural product leads, *J. Nat. Prod.* 67 (2004) 273–283.
- [5] K.W. Kohn, Y. Pommier, Molecular and Biological Determinants of the cytotoxic actions of Camptothecins Perspective for the Development of New Topoisomerase I Inhibitors, *Ann. N. Y. Acad. Sci.* 922 (2000) 11–26.
- [6] L. Wang, S. Xie, L. Ma, Y. Chen, W. Lu, 10-Boronic acid substituted camptothecin as prodrug of SN-38, *Eur. J. Med. Chem.* 116 (2016) 84–89.
- [7] F. Nie, J. Cao, J. Tong, M. Zhu, Y. Gao, Z. Ran, Role of Raf-kinase inhibitor protein in colorectal cancer and its regulation by hydroxycamptothecin, *J Biomed Sci*, 22 (2015) 56.
- [8] Z.F. Yuan, Y.M. Tang, X.J. Xu, S.S. Li, J.Y. Zhang, 10-Hydroxycamptothecin induces apoptosis in human neuroblastoma SMS-KCNR cells through p53, cytochrome c and caspase 3 pathways, *Neoplasma*, 63 (2016) 72-79.
- [9] X. Zhang, J. Jiang, B. Xu, Differentiation-inducing action of 10-hydroxycamptothecin on human hepatoma Hep G2 cells, *Acta Pharmacologica Sinica*, 21 (2000) 364-368.
- [10] S.L. Shao, W.W. Zhang, W. Zhao, G.H. Wu, Apoptosis of Human Leukemia Cell Line K562 Cells Induced by Hydroxycamptothecin, *Advanced Materials Research*, 535 (2012) 2420-2424.
- [11] W. Hu, C. Zhang, Y. Fang, C. Lou, Anticancer properties of 10-hydroxycamptothecin in a murine melanoma pulmonary metastasis model in vitro and in vivo, *Toxicology in Vitro*, 25 (2011) 513-520.
- [12] G. Meng, W. Wang, K. Chai, S. Yang, F. Li, K. Jiang, Combination treatment with triptolide and hydroxycamptothecin synergistically enhances apoptosis in A549 lung adenocarcinoma cells through PP2A-regulated ERK, p38 MAPKs and Akt signaling pathways, *Int J Oncol*, 46 (2015) 1007-1017.
- [13] Z. Liu, H. Li, Y. Fan, Y. Liu, S. Man, P. Yu, W. Gao, Combination treatment with Rhizoma Paridis and Rhizoma Curcuma longa extracts and 10-hydroxycamptothecin enhances the antitumor effect in H22 tumor model by increasing the plasma concentration, *Biomedicine & pharmacotherapy = Biomedecine & pharmacotherapie*, 83 (2016) 627-634.
- [14] Z. Liu, Q. Zheng, W. Chen, M. Wu, G. Pan, K. Yang, X. Li, S. Man, Y. Teng, P. Yu, W. Gao, Chemosensitizing effect of Paris Saponin I on Camptothecin and 10-hydroxycamptothecin in lung cancer cells via p38 MAPK, ERK, and Akt signaling pathways, *Eur. J. Med. Chem.* In Press (2016) DOI: 10.1016/j.ejmech.2016.09.066
- [15] J. Fassberg, V.J. Stella, A kinetic and mechanistic study of the hydrolysis of camptothecin and some analogues, *J. Pharm. Sci.* 81 (1992) 676–684.
- [16] C.Y. Wang, X.D. Pan, H.Y. Liu, Z.D. Fu, X.Y. Wei, L.X. Yang, Synthesis and antitumor activity of 20-O-linked nitrogen-based camptothecin ester derivatives, *Bioorg. Med. Chem.* 12 (2004) 3657–3662.
- [17] H. Zhao, C. Lee, P. Sai, Y.H. Choe, M. Boro, A. Pendri, S. Guan, R.B. Greenwald, 20-O-Acylcamptothecin derivatives: evidence for lactone stabilization, *J. Org. Chem.* 65 (2000) 4601–4606.
- [18] B.R. Vishnuvajjala, Garzon-Aburbeh, A. US 4 943 579, (1990).
- [19] Z. Cao, N. Harris, A. Kozielski, D. Vardeman, J.S. Stehlin, B. Giovanella, Alkyl esters of camptothecin and 9-nitrocamptothecin: synthesis, in vitro pharmacokinetics, toxicity, and antitumor activity, *J. Med. Chem.* 41 (1998) 31–37.
- [20] Z. Cao, B.C. Giovanella, US 6 228 855, (2001).
- [21] R. Bhatt, P.D. Vries, J. Tulinsky, G. Bellamy, B. Baker, J.W. Singer, P. Klein, Synthesis and in Vivo Antitumor Activity of Poly(L-glutamic acid) Conjugates of 20(S)-Camptothecin, *J. Med. Chem.* 46 (2003) 190–193.
- [22] L.X. Yang, X.D. Pan, H.J. Wang, Novel camptothecin derivatives. Part I: oxyalkanoic acid esters of camptothecin and their in vitro and in

- vivo antitumor activity, *Bioorg. Med. Chem. Lett.* 12 (2002) 1241–1244.
- [23] M.J. Wang, Y.Q. Liu, L.C. Chang, C.Y. Wang, Y.L. Zhao, X.B. Zhao, K. Qian, X. Nan, L. Yang, X.M. Yang, H.Y. Hung, J.S. Yang, D.H. Kuo, M. Goto, S.L. Morris-Natschke, S.L. Pan, C.M. Teng, S.C. Kuo, T.S. Wu, Y.C. Wu, K.H. Lee, Design, synthesis, mechanisms of action, and toxicity of novel 20(S)-sulfonylamidine derivatives of camptothecin as potent antitumor agents, *J Med Chem.* 57 (2014) 6008–18.
- [24] Z.L. Song, M.J. Wang, L. Li, D. Wu, Y.H. Wang, L.T. Yan, S.L. Morris-Natschke, Y.Q. Liu, Y.L. Zhao, C.Y. Wang, H. Liu, M. Goto, H. Liu, G.X. Zhu, K.H. Lee, Design, synthesis, cytotoxic activity and molecular docking studies of new 20(S)-sulfonylamidine camptothecin derivatives, *Eur. J. Med. Chem.* 115 (2016) 109–120.
- [25] X.D. Pan, H.Y. Liu, P.Y. Sun, C.G. Zhu, J. Yang, K.H. Yuan, R. Han, Synthesis and antitumor activity of 20-*O*-linked camptothecin ester derivatives, *Acta Pharm. Sin.* 39 (2004) 591–597.
- [26] D.Z. Li, C.Y. Wang, X.D. Pan, H.Y. Liu, Z.D. Fu, S. Wu, Synthesis and antitumor activity of A-ring modified hexacyclic analogues of camptothecin, *Acta Pharm. Sin.* 40 (2005) 241–247.
- [27] D.Z. Li, Y. Li, X.G. Chen, C.G. Zhu, J. Yang, H.Y. Liu, X.D. Pan, Synthesis and antitumor activity of heterocyclic acid ester derivatives of 20S-camptothecins, *Chinese Chemical Letters*, 18 (2007), 1335–1338.
- [28] L. Ouyang, D. He, J. Zhang, G. He, B. Jiang, Q. Wang, Z. Chen, J. Pan, Y. Li, L. Guo, Selective bone targeting 5-fluorouracil prodrugs: synthesis and preliminary biological evaluation, *Bioorg. Med. Chem.* 19 (2011) 3750–3756.
- [29] X.D. Pan, R. Han, P.Y. Sun, Regioselective synthesis and cytotoxicities of camptothecin derivatives modified at the 7-, 10- and 20-positions, *Bioorg. Med. Chem. Lett.* 13 (2003) 3739–3741.
- [30] L.G. Laurence, D. Daniele, K. Robert, Homocamptothecin, an E-Ring Modified Camptothecin with Enhanced Lactone Stability, Retains Topoisomerase I-targeted Activity and Antitumor Properties, *Cancer Research* 59 (1999) 2939–2943.
- [31] G.J. Creemers, B. Lund, J. Verweij, Topoisomerase I inhibitors: topotecan and irinotecan, *Cancer Treat Rev.* 20 (1994) 73–96.
- [32] Z.Y. Miao, L.J. Zhu, G.Q. Dong, C.L. Zhuang, Y.L. Wu, S.Z. Wang, Z.Z. Guo, Y. Liu, S.C. Wu, S.P. Zhu, K. Fang, J.Z. Yao, J. Li, C.Q. Sheng, W.N. Zhang, A New Strategy To Improve the Metabolic Stability of Lactone: Discovery of (20S, 21S)-21-Fluorocamptothecins as Novel, Hydrolytically Stable Topoisomerase I Inhibitors, *J. Med. Chem.* 56 (2013) 7902–7910.
- [33] G. Dong, S. Wang, Z. Miao, J. Yao, Y. Zhang, Z. Guo, W. Zhang, C. Sheng, New tricks for an old natural product: Discovery of highly potent evodiamine derivatives as novel antitumor agents by systemic structure–activity relationship analysis and biological evaluations, *J. Med. Chem.* 55 (2012) 7593–7613.
- [34] Y. Jiao, H. Liu, M. Geng, W. Duan, Synthesis and antitumor activity of 10-arylcampthothecin derivatives, *Bioorg Med Chem Lett.* 21 (2011) 2071–2074.
- [35] Z.N. Oltvai, C.L. Milliman, S.J. Korsmeyer, Bcl-2 heterodimerizes in vivo with a conserved homolog, bax, that accelerates programmed cell death, *Cell* 74 (1993) 609–619.
- [36] X.M. Yin, Z.N. Oltvai, S.J. Korsmeyer, Bhl and bh2 domains of bcl-2 are required for inhibition of apoptosis and heterodimerization with bax, *Nature* 369 (1994) 321–323.
- [37] P. Skehan, R. Storeng, D. Scudiero, A. Monks, J. McMahon, D. Vistica, J.T. Warren, H. Bokesch, S. Kenney, M.R. Boyd, New colorimetric cytotoxicity assay for anticancer-drug screening, *J. Natl. Cancer Inst.* 82 (1990) 1107–1112.
- [38] Z. Miao, C. Sheng, W. Zhang, H. Ji, J. Zhang, L. Shao, L. You, M. Zhang, J. Yao, X. Che, New homocamptothecins: Synthesis, antitumor activity, and molecular modeling, *Bioorg. Med. Chem.* 16 (2008) 1493–1510.
- [39] C. Zhuang, Z. Miao, L. Zhu, G. Dong, Z. Guo, S. Wang, Y. Zhang, Y. Wu, J. Yao, C. Sheng, W. Zhang, Discovery, synthesis, and biological evaluation of orally active pyrrolidone derivatives as novel inhibitors of p53–MDM2 protein–protein interaction, *J. Med. Chem.*

55 (2012) 9630–9642.

ACCEPTED MANUSCRIPT



Scheme 1. Synthesis of **5a–e** & **6–20**. Reagents and conditions: (i) 1. BrCH₂COOH or ClCH₂COOH / KOH / H₂O, 60°C; 2. HCl / r.t. (ii) RCH₂COOH (**5a–e**) / EDCI / DMAP / Pyridine (dried), r.t.

Table 1

Cytotoxicity of substituted uracil-1'(N)-acetic acid esters of CPTs against five human tumor cell lines

	IC ₅₀ (μM)				
	A549	Bel 7402	BGC-823	HCT-8	A2780
CPT	0.006	0.014	0.057	0.024	0.029
TPT	0.007	0.100	0.078	0.022	0.078
6	0.046	0.018	0.017	0.014	0.160
7	0.126	0.086	0.064	0.109	0.068
8	0.054	0.017	0.016	0.013	0.110
9	0.048	0.012	0.016	0.006	0.160
10	6.400	3.283	7.891	0.957	0.750
11	0.065	0.014	0.017	0.002	0.086
12	0.027	0.014	0.032	0.007	0.147
13	0.038	0.012	0.017	0.002	0.670
14	0.088	0.012	0.031	<0.002	0.182
15	0.710	4.510	2.573	0.586	0.669
16	0.051	0.018	0.017	0.014	0.073
17	0.081	0.016	0.017	0.013	0.115
18	0.075	0.016	0.017	0.013	0.221
19	0.090	0.013	0.015	0.013	0.183
20	0.117	0.013	0.016	0.014	0.200

A549: human lung cancer; Bel7402: human liver cancer; BGC-823: human stomach cancer; HCT-8: human colon cancer ; A2780: human ovarian cancer.

Table 2

Preliminary in vivo antitumor activity of substituted uracil-1'(N)-acetic acid ester analogues of CPTs against mouse liver tumor model (H22) (ip)

Group	Dose	Number	BW ^a /g		TW ^b /g	TIR ^c %	P value ^f
	mg/kg		d0/dn	d0			
Control	NS	11/11	21.7	32.5	2.69	-	-
Paclitaxel	24×3 ^d	10/9	21.8	18.9	0.70	73.85	<0.01
9	40×2 ^e	10/10	22.2	32.1	2.52	6.39	<0.01
12	40×2 ^e	10/10	21.8	27.3	1.14	57.51	<0.01
13	40×2 ^e	10/10	21.6	27.0	1.45	46.21	<0.01
16	40×2 ^e	10/10	22.2	32.0	2.39	11.00	<0.01

^aBW: Body weight; ^bTW: Tumor weight; ^cTIR: Tumor inhibitory rate; ^d: 24mg/kg in dose for every 3 days and totally for 3 times; ^e: 40mg/kg in dose for the first day and the 5 days later and totally for twice; ^fP: Significant difference compared to control group.

Table 3

Further *in vivo* antitumor activity of substituted uracil-1'(N)-acetic acid ester analogues of CPTs against mouse liver tumor model (H₂₂) for doses (ip)

Group	Dose	Number d0/dn	BW ^a /g		TW ^b /g	TIR ^c %	P value ^d
	mg/kg		d0	dn			
Control	NS	9/9	20.6	31.1	3.63	-	-
Cyclophosphamide	100×2	9/8	20.4	22.9	0.23	93.66	<0.01
12	100×1	10/8	20.6	29.8	2.21	39.12	<0.05
12	60×2	10/10	20.6	27.2	1.29	64.46	<0.01
13	100×1	10/6	20.8	25.2	1.50	58.68	<0.01
13	60×2	10/7	20.7	26.2	0.85	76.58	<0.01

^aBW: Body weight; ^bTW: Tumor weight; ^cTIR: Tumor inhibitory rate; ^dP: Significant difference compared to control group.

Table 4

Further in vivo antitumor activity of **12** against nude mice human gastric cancer model (BGC-823) for doses by weights (ip)

Group	Dose	Number	BW ^a /g		TW ^b /g	TIR ^c %	P value ^d
	mg/kg	d0/dn	d0	dn			
Control	NS	8/8	20.0	23.6	3.35	-	-
Irinotecan	50×2	8/8	19.8	20.5	0.18	94.10	<0.001
12	60×2	8/8	19.9	21.9	0.14	95.97	<0.001
12	30×2	8/8	20.5	19.1	0.35	89.70	<0.001

^aBW: Body weight; ^bTW: Tumor weight; ^cTIR: Tumor inhibitory rate; ^dP: Significant difference compared to control group.

Table 5

Further in vivo antitumor activity of **12** against nude mice human gastric cancer model (BGC-823) for doses by tumor volumes (ip)

Group	Dose	Number	BV ^a /g		RTV ^b /g	T/C ^c %	P value ^d
	mg/kg	d0/dn	d0	dn			
Control	NS	8/8	119	2533	22.73	-	-
Irinotecan	50×2	8/8	115	147	1.25	5.48	<0.001
12	60×2	8/8	114	143	1.26	5.54	<0.001
12	30×2	8/6	125	334	2.87	12.65	<0.001

^aBV: Body volume; ^bRTV: Tumor volume; ^cT/C: Testing group compared to control group; ^dP: Significant difference compared to control group.

Table 6

Further in vivo antitumor activity of **12** against nude mice liver tumor model (Be1-7402) for doses by weights (ip)

Group	Dose	Number	BW ^a /g		TW ^b /g	TIR ^c %	P value ^d
	mg/kg	d0/dn	d0	dn			
Control	NS	8/8	18.6	14.5	0.57	-	-
TPT	5×2	8/7	19.8	14.0	0.31	45.48	<0.05
12	60×2	8/8	18.9	14.0	0.11	81.45	<0.001
12	30×2	8/6	18.6	14.4	0.21	62.60	<0.05

^aBW: Body weight; ^bTW: Tumor weight; ^cTIR: Tumor inhibitory rate; ^dP: Significant difference compared to control group.

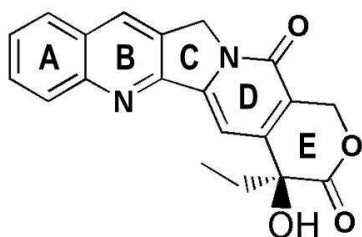
Table 7

Further in vivo antitumor activity of **12** against nude mice liver tumor model (Be1-7402) for doses by tumor volumes (ip)

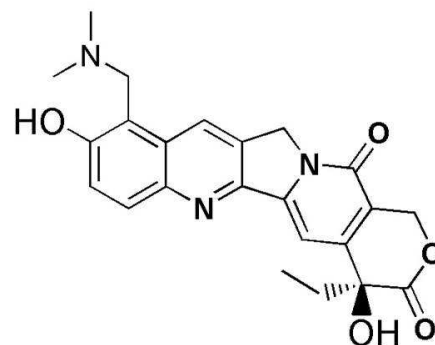
Group	Dose	Number	BV ^a /g		RTV ^b /g	T/C ^c %	P value ^d
	mg/kg	d0/dn	d0	dn			
Control	NS	8/8	113	511	4.44	-	-
TPT	5×2	8/7	115	302	2.61	58.80	<0.01
12	60×2	8/8	115	127	1.09	24.53	<0.001
12	30×2	8/6	119	231	1.87	41.17	<0.01

^aBV: Body volume; ^bRTV: Tumor volume; ^cT/C: Testing group compared to control group; ^dP: Significant difference compared to control group.

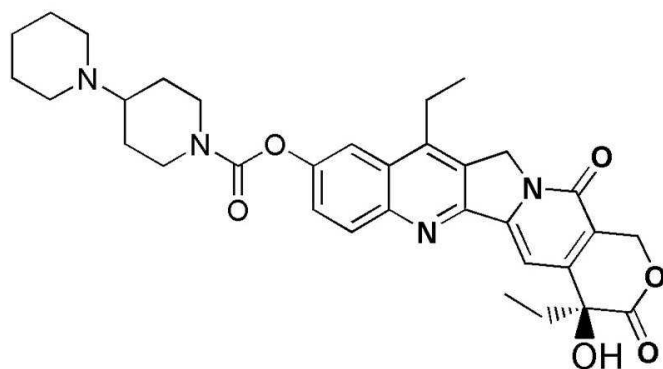
Li. Fig1



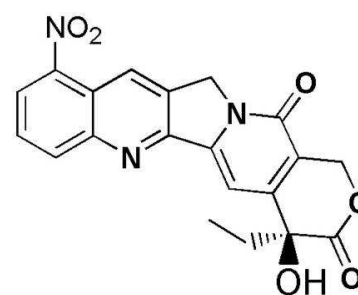
Camptothecin(1)



Topotecan(2)



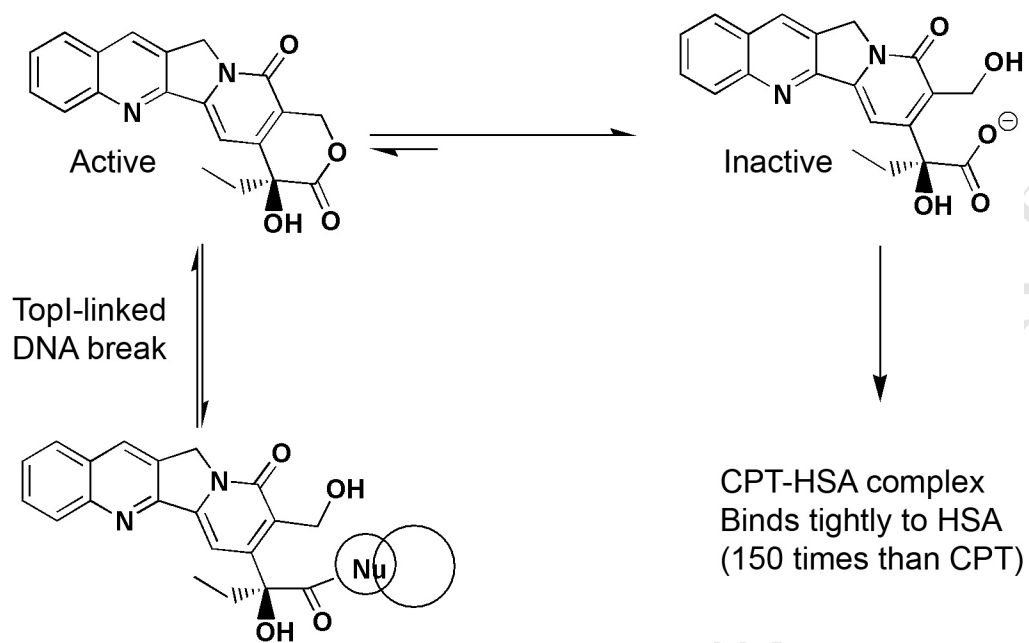
Irinotecan(3)



Rubitecan (9-nitrocamptothecin,4)

ACCEPTED

Li. Fig2

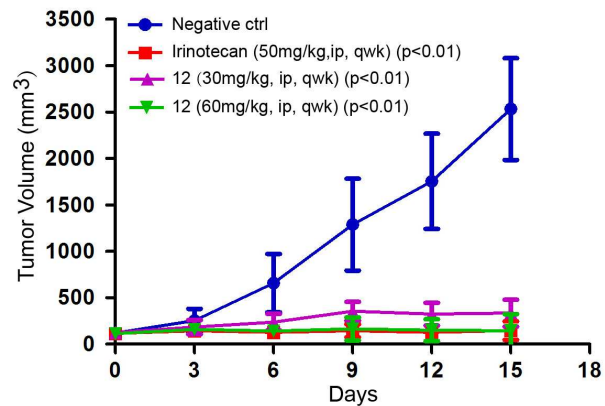


Li. Fig3

A



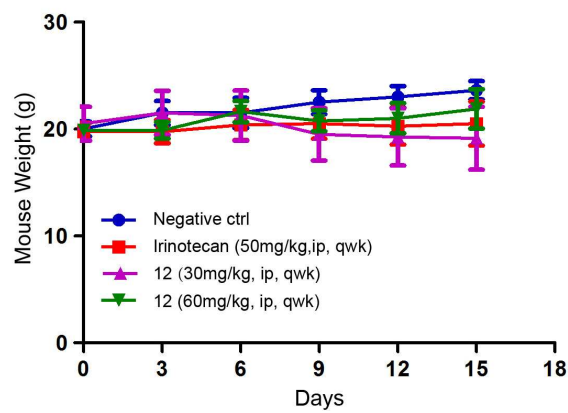
B



C

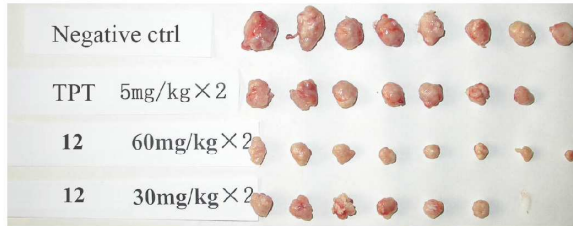


D

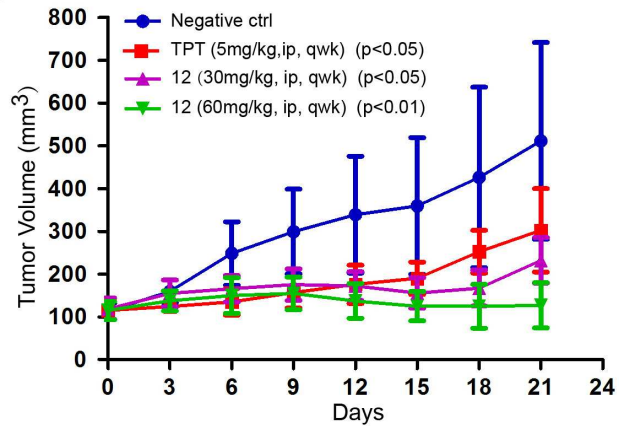


Li. Fig4

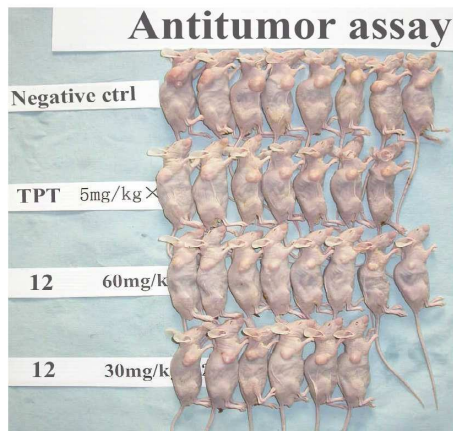
A



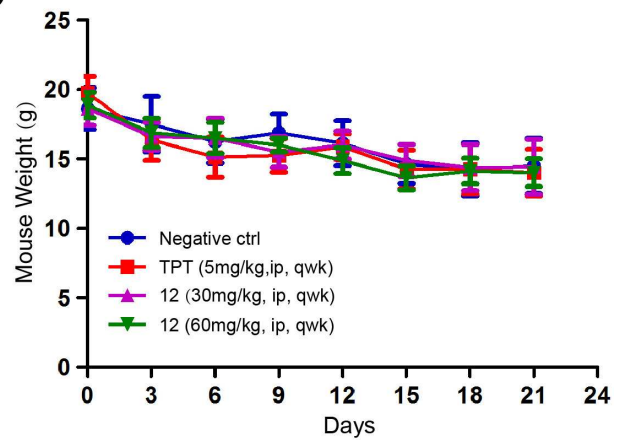
B



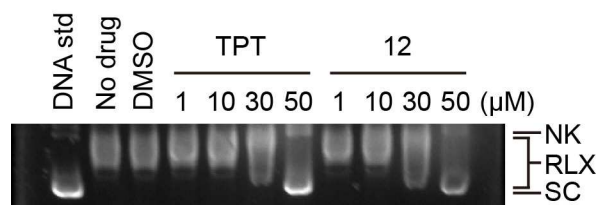
C



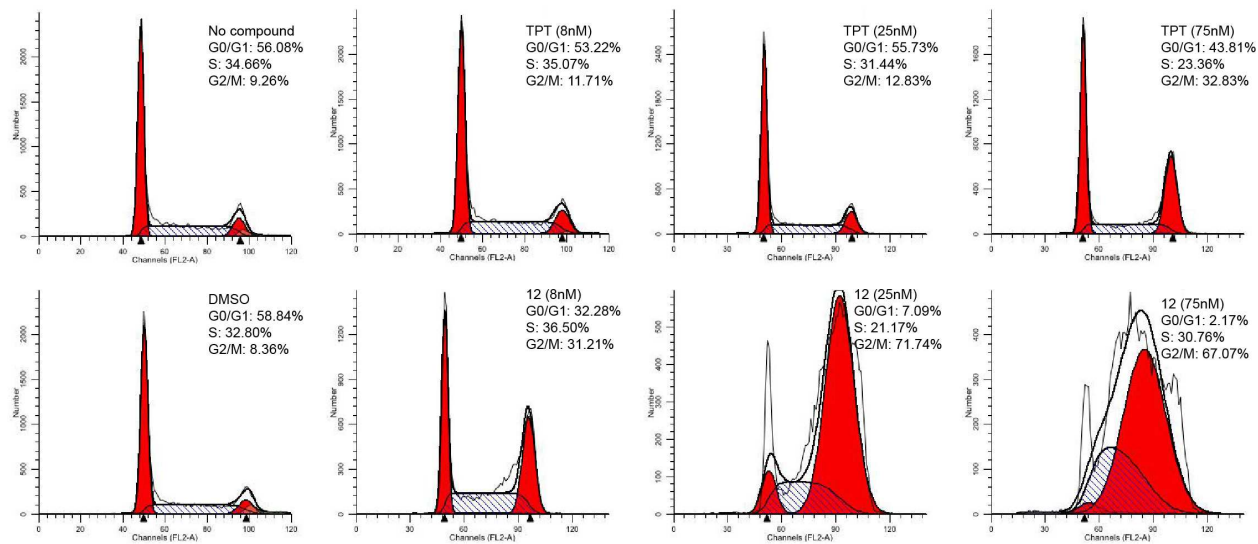
D



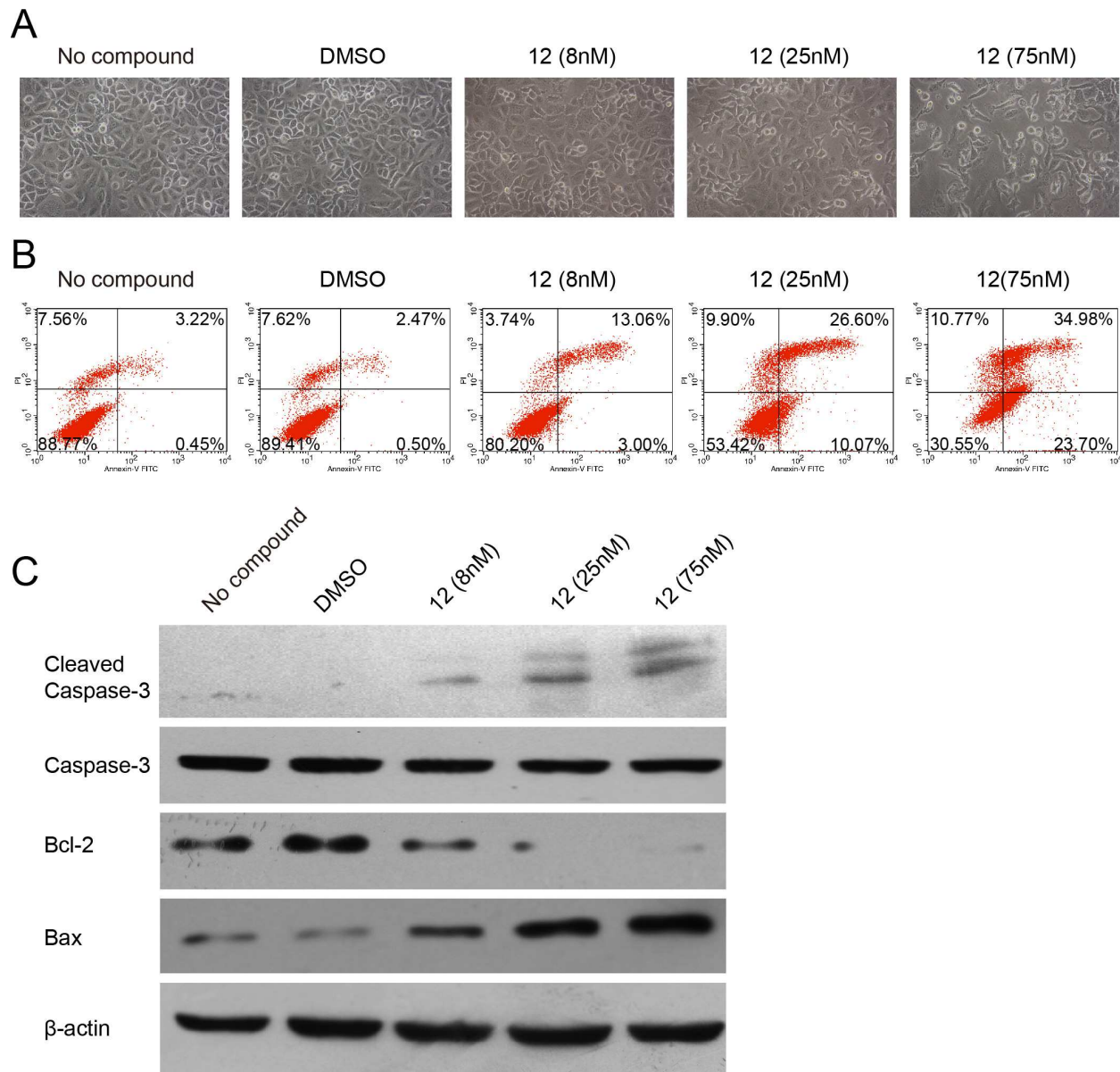
Li. Fig5



Li. Fig6



Li. Fig7



Li. Fig 8

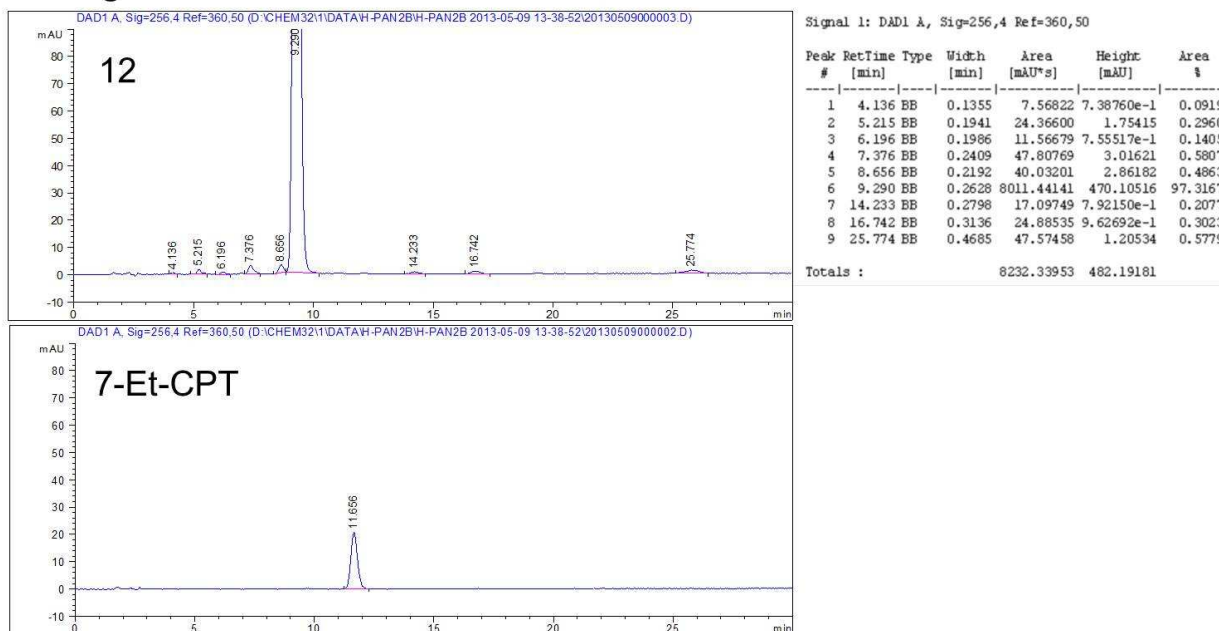


Figure 1. Structures of camptothecin (1), topotecan (2), irinotecan (3), rubitecan (4).

Figure 2. Structure, activity and reactivity of camptothecin.

Figure 3. *In vivo* antitumor activity of **12** against human gastric cancer model (BGC-823) in nude mice compared to irinotecan. (A) Image of the internal tumor tissues after anatomy; (B) Image of tumor-bearing mice before anatomy; (C) Relationship curves of tumor volumes at various times (0, 3, 6, 9, 12, and 15 days) after intraperitoneally; (D) Relationship curves of mice weights at various times (0, 3, 6, 9, 12, and 15 days) after intraperitoneally.

Figure 4. *In vivo* antitumor activity of **12** against liver tumor model (Bel-7402) in nude mice compared to TPT. (A) Image of the internal tumor tissues after anatomy; (B) Image of tumor-bearing mice before anatomy; (C) Relationship curves of tumor volumes at various times (0, 3, 6, 9, 12, 15, 18, and 21 days) after intraperitoneally; (D) Relationship curves of mice weights at various times (0, 3, 6, 9, 12, 15, 18, and 21 days) after intraperitoneally.

Figure 5. Topo I-mediated plasmid DNA pcmv-6 relaxation assay of **12** and TPT. Pcmv-6 DNA was incubated with Top I in the presence or absence of indicated drugs at 37 °C for 30 minutes and terminated by the addition of 10% sodium dodecylsulfate. The mixtures then were analyzed on a 1% agarose gel. TPT was used as reference drug. The position of supercoiled DNA (SC) and relaxed DNA (RLX) were indicated.

Figure 6. Cell cycle alterations in response to compounds TPT and **12** treatment. A549 cells were treated with TPT and **12** for 24 h. Cell cycle profiles and the percentage of the cells in G0/G1, S, and G2 /M phases were analyzed by flow cytometry.

Figure 7. Induction of apoptosis by compound **12**. (A) Cells morphology of A-549 cells treated with compound **12**. A-549 cells were incubated in the absence or presence of **12** for 24 h. Morphological changes were observed under a phase-contrast microscope. (B) Percentages of apoptotic cells of A-549 cells treated with compound **12**. A-549 cells were treated without or with **12** for 24 h followed by FITC-annexin V with propidium iodide double staining. Percentages of apoptotic cells were analyzed by flow cytometry. (C) Compound **12** enhances apoptosis signal. A-549 cells were treated with **12** at concentration from 8 nM to 75 nM. Cells were harvested and lysed for the determination of cleaved Caspase-3, Caspase-3, and Bcl2/Bax using Western blot analysis.

Figure 8. Reverse-phase HPLC chromatograms of compound **12** and 7-Et-CPT, by monitoring the UV/Vis absorption at 256 nm. The retention times of compound **12** and 7-Et-CPT are 9.29 min and 11.66 min, respectively.

Highlights

- 20(*S*)-uracil-1'(*N*)-acetic acid CPT-ester derivatives were synthesized.
- Several analogs exhibited superior cytotoxicity compared to CPT and TPT.
- **12** possessed higher in vivo antitumor activity and lower toxicity than TPT.
- The mechanism study revealed that **12** was a Top I inhibitor as same as TPT.
- **12** is a new class of antitumor clinical trial drug candidate of CPTs.